Journal of Water Process Engineering 64 (2024) 105744

Contents lists available at ScienceDirect

Journal of Water Process Engineering

journal homepage: www.elsevier.com/locate/jwpe

Superoxide radicals dominated hydrogen peroxide activation using BiOI for boosting Fenton-like catalytic degradation of bisphenol A

Jinghao Huo [a,b], Xin Nie [b,*], Yanfei Yin [a], Quan Wan [b,c], Jukun Xiong [d], Huixian Shi [a,*]

[a] College of Material Science and Engineering, Taiyuan University of Technology, Taiyuan 030024, China
[b] State Key Laboratory of Ore Deposit Geochemistry, Institute of Geochemistry, Chinese Academy of Sciences, Guiyang 550081, China
[c] CAS Center for Excellence in Comparative Planetology, Hefei 230026, China
[d] Guangzhou Key Laboratory of Environmental Catalysis and Pollution Control, Guangdong Technology Research Center for Photocatalytic Technology Integration and Equipment Engineering, School of Environmental Science and Engineering, Guangdong University of Technology, Guangzhou 510006, China

ARTICLE INFO

Editor: Akeem Oladipo

Keywords:
BiOI
Fenton-like catalytic
Superoxide radicals
Bisphenol A
Degradation mechanism

ABSTRACT

Herein, flower-like BiOI micro-spherulites were successfully prepared via a solvothermal method, and it exhibited a remarkably Fenton-like catalytic efficacy in the degradation of BPA under dark condition without additional energy input. BiOI can function as an electron-poor center, facilitating the activation of H_2O_2 into $\bullet O_2^-$, while simultaneously serving as an electron-rich center to reduce dissolved O_2 to $\bullet O_2^-$. This electron-rich and electron-poor centers of BiOI synergistically enhance the $\bullet O_2^-$ generation for highly Fenton-like catalytic performance. Moreover, the removal performance of BPA demonstrated a significant pH dependency, and the presence of low concentrations of halide ions and humic acid did not exhibit noticeable inhibitory effect on the degradation of BPA. Additionally, several intermediates have been identified to propose a comprehensive degradation mechanism for BPA. This study presents a novel BiOI Fenton-like catalytic system for the purification of recalcitrant organic pollutants in wastewater.

1. Introduction

Bisphenol A (BPA, 2, 2-bis (4-hydroxyphenyl) propane) is an important industrial raw material primarily employed in the production of polycarbonate plastics, epoxy resins, and polysulfonate resins. It finds extensive application as liners for various products such as mineral water bottles, food containers, electronic components, and so on. Owing to its inherent structural stability and limited biodegradability [1,2], BPA has received considerable attention about its environmental fate due to its endocrine disrupting activity, carcinogenesis and genotoxicity, which could pose a serious health risk to aquatic organisms even at trace concentration level, ultimately affecting ecological environment and human health through bioaccumulation of the food chain [1–4]. Therefore, the efficient elimination of BPA from wastewater and natural water systems holds substantial implications for safeguarding environmental and public health. However, conventional wastewater treatment methods including adsorption, biological treatment, chemical treatment and membrane filtration exhibit inherent limitations in effectively eliminating BPA. These technologies encounter a range of inevitable impediments and limitations, such as suboptimal removal efficiency, secondary pollution by toxic byproducts, high costs, recalcitrance and demanding energy or labor intensive [2,3,5,6]. Therefore, significant endeavors have been dedicated to the development of novel technologies aimed at efficiently eradicating BPA from aqueous environments.

Advanced oxidation processes (AOPs) are recognized as efficient and environmentally friendly technologies for the removal of refractory pollutants. This is due to their ability to generate highly reactive oxygen species (ROSs), such as $\bullet OH$, $\bullet SO_4^-$, $\bullet O_2^-$, which can effectively react with various recalcitrant organic compounds. AOPs have the potential to completely transform these compounds into non-toxic, low molecular products or even mineralize them into CO_2 and H_2O [5,7]. Among them, the Fenton or Fenton-like process has been undoubtedly recognized as one of the most powerful and promising AOPs techniques for effectively decontaminating wastewater containing organic pollutants for its high efficiency, economic benefits and widely application in various contexts [5,8,9]. Unfortunately, the practical application of the conventional homogeneous Fenton process is still hindered by several limitations, including the generation of substantial quantities of ferric hydroxide sludge and a narrow operational pH range (typically 2.0–4.0) [7,10]. Alternatively, various transition-metal-based heterogeneous Fenton-like

* Corresponding authors.
E-mail addresses: niexin2004@163.com (X. Nie), shihuixian@tyut.edu.cn (H. Shi).

https://doi.org/10.1016/j.jwpe.2024.105744
Received 25 April 2024; Received in revised form 26 June 2024; Accepted 2 July 2024

catalysts have been widely developed and are thus considered highly promising candidates for homogeneous Fenton reaction due to their ability to flexibly adjust surface properties and abundant availability [10]. However, the activation of H_2O_2 by most heterogeneous Fenton catalysts primarily occurs through redox reactions at the surface metal sites in the solid-liquid interface. This process can result in a significant release of undesirable metal ions from the catalyst surface into the reaction solution as free metal ions, thereby potentially causing direct or indirect toxicity to aquatic organisms and even humans. In addition, heterogeneous Fenton catalysts exhibit subpar catalytic performance in neutral conditions and demonstrate low efficiency in utilizing H_2O_2 [3,10,11]. Most importantly, the majority of previous studies pertaining to heterogeneous Fenton or Fenton-like catalytic processes have predominantly relied on the production of short-lived •OH radicals with a limited half-life of 1 μs, which can be easily consumed by complex water matrices. However, these limitations could be alleviated by developing a heterogeneous catalyst capable of selectively generating longer-lived and highly efficient ROSs through enhanced heterogeneous Fenton or Fenton-like catalytic activity. As an enduring and exceptionally active oxygen species, $•O_2^-$ can simultaneously reduce and oxidize organic pollutants. Its higher half-life span permits long diffusion distance and tremendous interaction between $•O_2^-$ and pollutants [12]. It is feasible to selectively activate H_2O_2 into $•O_2^-$ by constructing a Fenton-like catalytic system featuring electron-rich and electron-poor dual-reaction centers on the surface of catalyst [3,11].

Layered bismuth-based materials, such as bismuth oxyhalides (BiOX , X = Cl, Br, I), have received considerable attentions for energy conversion and environment remediation due to their unique two-dimensional layered crystal structure, fine-tuned surface properties and photocatalytic activity [13,14]. However, low utilization of solar energy and rapid recombination rate of photogenerated charge carrier still inhibits their practical applications. Various strategies, including elemental doping, defect engineering, facet control, bismuth-rich and heterojunction have been devoted to enhance their catalytic activity [14–16]. Recently, many investigations have demonstrated that electron-poor oxygen vacancies on the surface of BiOI could effectively activate H_2O_2 to generate ROSs without light irradiation, implying that BiOI is likely to be used as a light-free Fenton-Like catalyst for the efficient removal of organic pollutants [3]. However, limited studies have paid attention to selectively activate H_2O_2 to $•O_2^-$ rather than to •OH, and the mechanism for H_2O_2 activation to generate $•O_2^-$ have not been specifically revealed.

Herein, in present work, as shown in Scheme 1, the heterogeneous Fenton-like catalysts of flower-like BiOI micro-spherulites could efficiently and selectively activate H_2O_2 to $•O_2^-$, were successfully constructed by a solvothermal method. BPA was selected for the evaluation of the Fenton-like catalytic activity of BiOI. The catalysts exhibited excellent Fenton-like catalytic activity and showed good degradation performance toward BPA with highly effective H_2O_2 activation by the electron-poor centers at the catalyst surface. The effects of various solution chemistry conditions (pH, H_2O_2 concentration, BPA concentration, halide ions, humic acid) on the Fenton-like catalytic degradation of BPA were systematically investigated. The contribution of ROSs for the BPA degradation and the detailed degradation mechanisms of BPA underpinning the identification of degradation intermediates during the Fenton-like catalytic process were also elucidated. These findings suggest that the flower-like BiOI micro-spherulites exhibit significant potential for the remediation of water contaminated with BPA.

2. Experimental section

2.1. Synthesis and characterization of BiOI

BiOI microspheres were synthesized by a facile solvothermal method [17,18]. The crystallinity and catalytic activity of BiOI was tuned by adjusting the solvothermal reaction temperature. In a typical procedure, 4 mM KI was dissolved in 30 mL ethylene glycol, and then added dropwise into 30 mL ethylene glycol containing 4 mM $Bi(NO_3)_3·5H_2O$ under vigorous stirring at 25 °C for 30 min. The mixture was then transferred into a 100 mL Teflon-lined stainless autoclave, and kept at selected temperatures (120, 160, 180, 200 and 220 °C) for 12 h. After naturally cooling down to room temperature, the precipitates were collected by centrifugation and washed with deionized water and ethanol for three times. Finally, the as-synthesized samples were dried at 80 °C. The as-prepared samples were defined as T-120, T-160, T-180, T-200 and T-220 based on their solvothermal reaction temperature.

The crystal phase composition and crystallinity were characterized using X-ray diffraction (XRD, Empyrean, PANalytical B·V) operating with Cu-Ka radiation. The elemental composition was characterized using X-ray photoelectron spectroscopy (XPS, Thermo Fisher K-Alpha) with monochromated Al Kα (1486.6 eV) source operated at 110 W, and the XPS spectra was calibrated by C 1 s peak at 284.8 eV. The morphologies of the samples were observed using transmission electron microscope (TEM, Tecnai G2 F20 S-Twin, FEI Company) and Field emission scanning electron microscopy (FESEM, Scios, FEI Company) with an acceleration voltage of 30.0 kV. The zeta potentials of samples were measured by a multi angle particle size and highly sensitive zeta potential analyzer (Omni, Brookhaven).

2.2. Catalytic degradation experiments of BPA

Fenton-like catalytic activity of BiOI was evaluated by H_2O_2 activation under dark environmental condition without additional energy input (such as light, electricity and ultrasound irradiation). In a typical batch experiment, 0.05 g catalyst was dispersed in 100 mL BPA solution with various initial pH and concentrations, and the mixture is stirred at

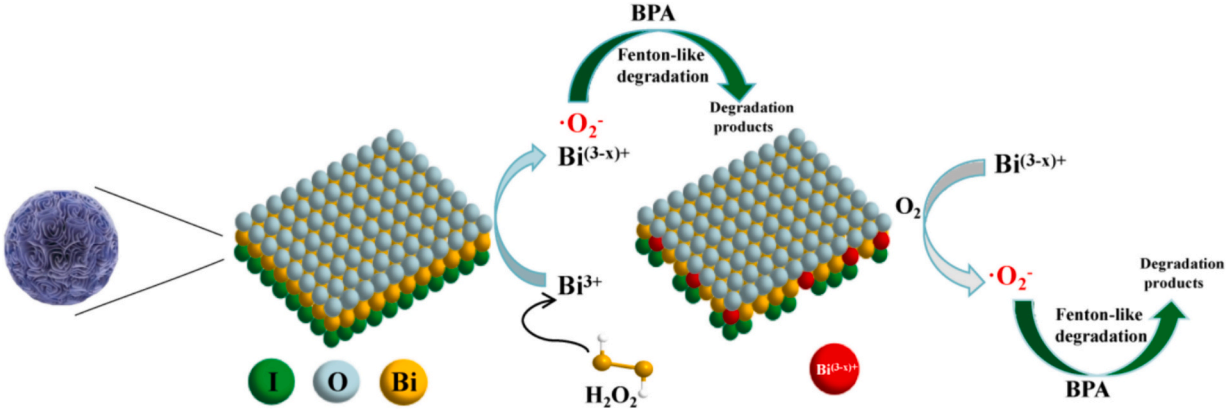

Scheme 1. Schematic illustration of $•O_2^-$ dominated H_2O_2 activation using BiOI for boosting Fenton-like catalytic degradation of BPA.

room temperature for about 30 min to establish the adsorption-desorption equilibrium between BPA and the catalyst. Then, in the case of continuous agitation, a certain volume of H_2O_2 solution (2 mL, 100 mmol/L) was added to the above suspension to trigger Fenton-like reaction. About 3 mL of solution was sampled at given time intervals and transferred into the ethanol solution to cease the Fenton-like reaction immediately. After filtration with 0.45 μm Millipore filter, the supernatant was used for BPA concentration measurement by high pressure liquid chromatography (HPLC, Agilent 1200) at the wavelength of 275 nm with a dual absorbance detector (DAD) detector equipped with a Kromasil ODS (5 μm, 4.6 mm × 150 mm) reverse-phase column. HPLC tandem mass spectrometry (HPLC/MS/MS, Q Exactive, Thermo Fisher Scientific) was used to identify intermediates during BPA degradation. The solid specimens were dried at 30 °C and used to measure the surface chemical species by XPS. The detailed information is provided in the Supporting information.

The quenching experiments were carried out to identify the main ROSs in the Fenton-like system by adding 10 mmol/L isopropanol (IPA), Tert-butanol (TBA), L-histidine, and p-benzoquinone (BQ) as scavengers of $\bullet OH_{bulk}$ ($\bullet OH$ in solution), total $\bullet OH$ ($\bullet OH$ in solution and $\bullet OH$ adsorbed on the surface of BiOI), $^1O_2$, and $\bullet O_2^-$, respectively. Free radicals ($\bullet OH$, $^1O_2$, and $\bullet O_2^-$) were measured using an electron spin-resonance (ESR) spectrometer (EMXPLUS10/12, Bruker). 5, 5-dimethyl-L-pyrroline-*N*-oxide (DMPO) and 4-amino-2,2,6,6-tetramethylpiperidine (TEMP) trapped ESR signals were detected in different air saturated methanol/aqueous dispersions of the corresponding samples. Typically, in the presence or absence of H_2O_2, 5 mg of the catalyst sample was added to 10 mL of water (for detecting $\bullet OH$) or methanol (10 %/90 %, *V*/V, for detecting $\bullet O_2^-$). Then, 4 mL of the above suspension, 1 mL of DMPO or TEMP (100 mM) and H_2O_2 (100 mM, 0.1 mL) were mixed and held for 2 min. The solution was sucked into the capillary to carry out ESR detection.

3. Results and discussion

3.1. Structural and morphological characterization of BiOI catalysts

The influence of solvothermal temperature on the structural and morphological evolution of as-synthesized samples was systematically investigated within the temperature range of 120–220 °C. Fig. 1a demonstrates that the characteristic diffraction peaks at 9.7°, 19.4°, 24.3°, 29.6°, 31.7°, 33.2°, 45.4°, 46.5°, 51.3° and 55.2° were attributed to the (001), (002), (101), (102), (110), (111), (200), (201), (114) and (212) planes of BiOI (JCPDS No.10–0445), respectively [3]. When the solvothermal temperature was 120 °C, a weak characteristic diffraction peak at 22.6° could be observed, which was attributed to the (221) plane of Bi_2O_3 (JCPDS No.74–2351). When the solvothermal temperatures increased from 120 to 180 °C, the peak intensities of BiOI decreased gradually, indicating the reduction of crystallinity. This may be ascribed to the rapid crystal nucleation rate of BiOI at high solvothermal temperature. The diffraction peaks of metallic Bi appeared for the sample synthesized at 180 °C, indicating that partial BiOI dissociated and formed a composite of Bi/BiOI at high temperatures [1,19]. As the temperature further increased to 220 °C, the characteristic peaks of BiOI become much weaker, and the peak intensities of metallic Bi increased significantly. The characteristic diffraction peaks at 22.5°, 27.2°, 37.9°,

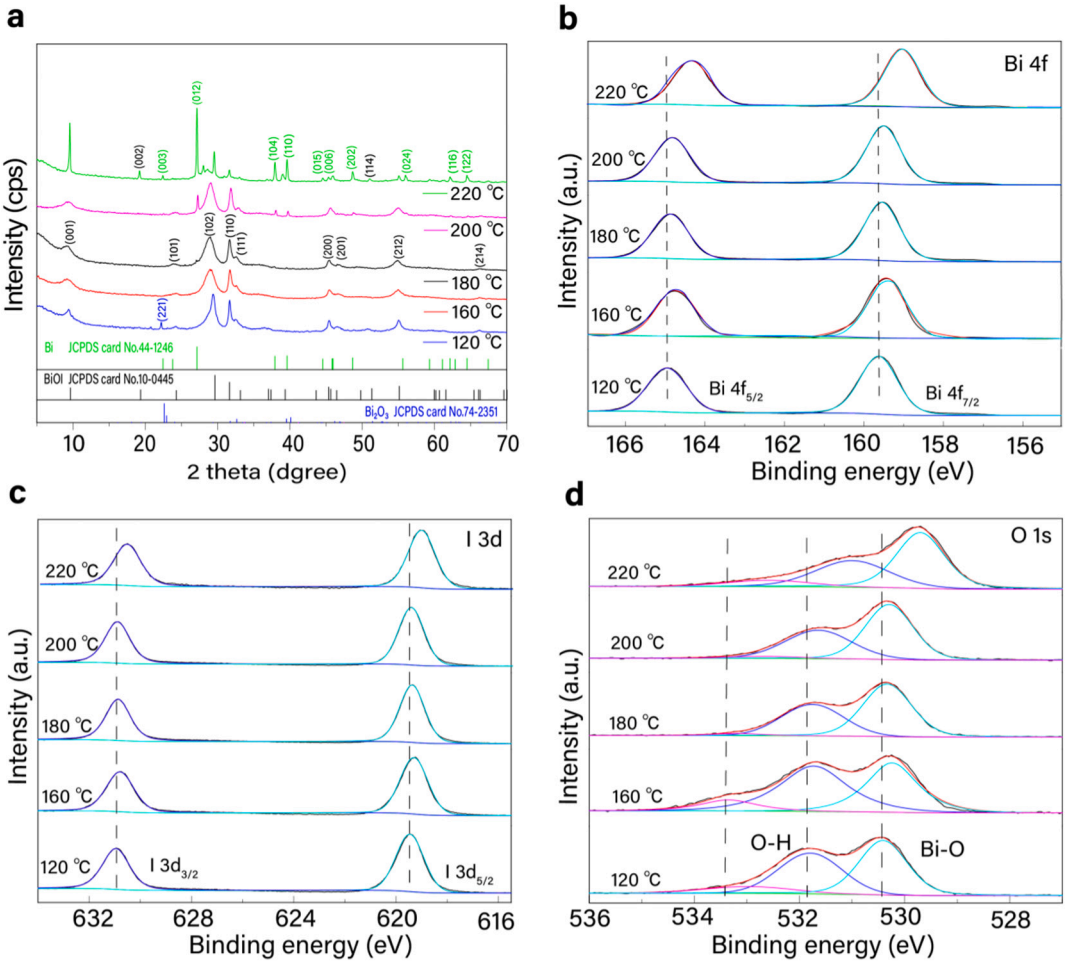

Fig. 1. XRD patterns (a), XPS spectra of Bi 4f (b), I 3d (c) and O 1s (d) for the catalysts prepared at different solvothermal temperatures.

39.6°, 44.6°, 46.0°, 48.7°, 55.6°, 62.2°, and 64.5° were attributed to the (003), (012), (104), (110), (015), (006), (202), (024), (116) and (122) planes of metallic Bi (JCPDS No. 44–1246).

The surface chemical composition and chemical states of the samples synthesized at various temperatures were examined using XPS spectrometry (Fig. 1b-d). When the solvothermal temperature was lower than 200 °C, the XPS spectra of the samples exhibited similar characteristics. The Bi 4f spectrum (Fig. 1b) exhibits two distinct peaks at 159.5 and 164.9 eV, corresponding to the Bi $4f_{7/2}$ and Bi $4f_{5/2}$ states for Bi^{3+}, respectively [20]. For the T-220 sample, the peaks of Bi^{3+} are located at 164.3 and 159 eV, which are lower than those of T-180 sample, indicating the possible appearance of $Bi^{(3-x)+}$ and oxygen vacancies on the surface of T-220 [20]. Furthermore, metallic Bi was not observed on the surface of T-220, but it appeared in the XRD pattern, indicating that metallic Bi was in the interior of the catalyst and coated with Bi_2O_3 due to the oxidation of the surface of metallic Bi. Fig. 1c depicts the high-resolution XPS spectrum for I 3d, wherein the presence of two prominent peaks at 619.4 and 630.9 eV can be attributed to the existence of I^- originating from BiOI [3]. As shown in the Fig. 1d, the O 1s XPS spectrum can be accurately fitted with three distinct peaks. The peaks observed at 530.4 and 531.7 eV correspond to the lattice Bi—O bond and O—H bond on the surface of sample, respectively, while the peak detected at 533.4 eV can be attributed to oxygen adsorbed on the surface [3]. The shift of peaks belonging to Bi, I and O for T-220 sample to low binding energy should be attributed to the presence of $Bi^{(3-x)+}$ and oxygen vacancies on the surface of T-220.

The surface morphologies and detailed microstructures of the as-prepared samples were characterized by FESEM (Fig. 2 (a-e)) and TEM (Fig. 2 (f-i)). At the solvothermal temperatures ranging from 120 to 180 °C, the BiOI exhibited typical morphologies consisting of 3D hierarchical micro-spherulites assembled from nanosheets, and the diameter of these micro-spherulites was approximately 3–4 μm. In addition, no significant morphological changes were observed within this temperature range. The microspheres underwent partial deformation at a temperature of 200 °C. Upon further increasing the temperature to 220 °C, the micro-spherulites vanished and a mixture of irregular flakes and bulk particles was obtained. As exhibited in Fig. 2f, the low-magnification TEM reveals the presence of a well-defined lamellar structure in the T-180 sample. Moreover, the high-resolution TEM (HRTEM) image (Fig. 2i) recorded from the blue circled area in Fig. 2f demonstrates distinct lattice fringes with a spacing of approximately 0.360 nm, corresponding to the crystallographic interplanar distances of BiOI along the (101) orientation. Fig. 2g illustrates that the T-220 sample comprises nanosheets adorned with a substantial quantity of nanoparticles on their surface. The corresponding HRTEM image is presented in Fig. 2h, revealing the presence of two distinct lattice fringes with d spacing values of approximately 0.300 and 0.298 nm, which can be confidently assigned to the (212) planes of Bi. This observation aligns well with the XRD findings, indicating that elevated solvothermal temperatures do not favor the formation of BiOI.

3.2. Fenton-like catalytic degradation of BPA by BiOI

The Fenton-like catalytic degradation performances of the as-prepared samples at different solvothermal temperatures were evaluated through H_2O_2 activation to degrade BPA. Adsorption capacity of BPA onto BiOI prepared at 180 °C was firstly investigated at different pH conditions without the addition of H_2O_2. As shown in Fig. S1a, under all tested pH conditions, negligible adsorption of BPA was observed within 90 min, indicating the low adsorption ability of BiOI. The zeta potential values of BiOI prepared at 180 °C exhibited a negative charge across all tested pH conditions (Fig. S1b), indicating the surface of BiOI was negatively charged. The pKa of BPA is 9.60, which normally formed BPA molecules and BPA^{2-} at low pH values and high pH values, respectively [21]. Therefore, due to the absence of electrostatic attraction between BiOI and BPA, the equilibrium adsorption capacity of BPA remains low under all tested pH conditions. Fig. 3a shows the Fenton-like catalytic degradation curves of BPA with an initial pH of 5.0 by the BiOI prepared at different solvothermal temperatures. The degradation rate of BPA exhibited a significant increase with the rise in solvothermal

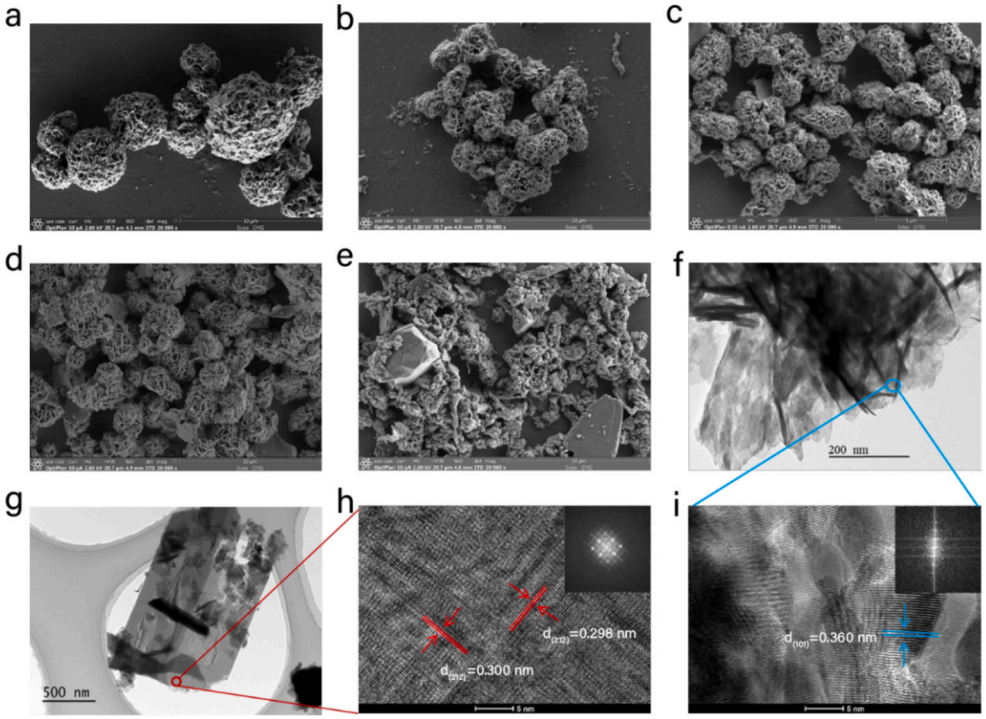

Fig. 2. FESEM images of the catalysts synthesized at different solvothermal temperatures: (a) 120 °C; (b) 160 °C; (c) 180 °C; (d) 200 °C; (e) 220 °C. Low-magnification TEM images (f) and high-magnification TEM (HRTEM) images of BiOI synthesized at 180 °C with corresponding Fast Fourier Transform (FFT) images (i); Low-magnification TEM images (g) and HRTEM images of BiOI synthesized at 220 °C with corresponding FFT images (h).

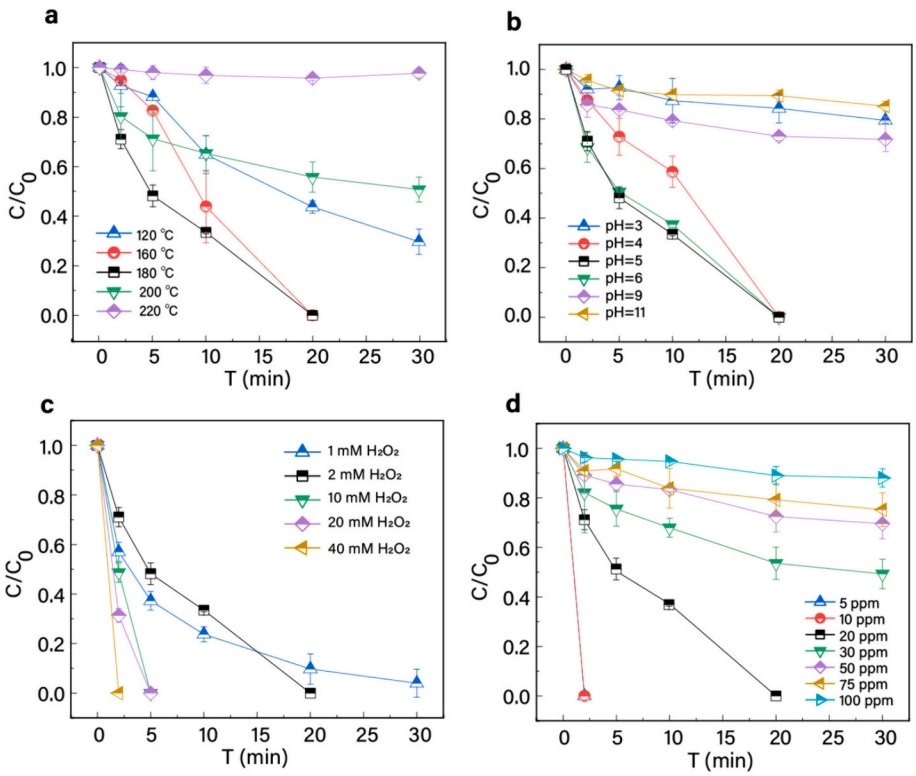

Fig. 3. Fenton-like catalytic degradation curves of BPA by the catalysts synthesized at different solvothermal temperatures (a); Fenton-like catalytic degradation of BPA by BiOI synthesized at 180 °C with different initial pHs (b), H_2O_2 dosages (c), and BPA concentrations (d). Fenton-like catalytic conditions: catalysts = 0.5 g/L, pH = 5.0, BPA = 20 mg/L, H_2O_2 = 2 mmol/L.

temperature from 120 to 180 °C. All BPA was completely eliminated within 20 min by the samples prepared at temperatures ranging from 160 to 180 °C. Notably, the sample prepared at 180 °C exhibited the most exceptional rate of BPA removal, indicating its superior Fenton-like catalytic performance. However, the degradation rate of BPA significantly decreased when the solvothermal temperature was increased to 200 °C, resulting in only approximately 50 % degradation efficiency after 30 min. Furthermore, negligible removal of BPA was observed when the solvothermal temperature reached 220 °C. This suggests that the sample prepared at a temperature of 220 °C is expected to exhibit catalytic inactivity in the Fenton-like reaction. Based on the aforementioned results, it is evident that the sample prepared at 180 °C exhibits the highest activation efficiency for H_2O_2 and demonstrates superior Fenton-like catalytic performance in degrading BPA, which might be closely related to the formation of small amounts of metallic Bi. Consequently, the BiOI synthesized at 180 °C was selected as the optimized catalyst for further investigations into BPA removal in subsequent experiments.

Solution initial pH commonly plays a crucial role in the Fenton-like catalytic reaction process [5]. To optimize the conditions for Fenton-like catalytic degradation of BPA by BiOI, we initially examined the effect of initial pH of the solution (ranging from 3.0 to 11.0) on the Fenton-like catalytic degradation process of BPA. As depicted in Fig. 3b, the Fenton-like degradation rates of BPA exhibited a noticeable acceleration as the pH increased from 3.0 to 4.0. Within the initial pH range of 4.0–6.0, complete removal of BPA could be achieved within a mere 20 min, with the highest degradation rate observed at an initial pH of 5.0. However, upon further elevation of the initial pH of solution, a significant decline in the degradation rate of BPA was evident. At initial pH values of 3.0, 9.0 and 11.0, the Fenton-like degradation rate of BPA by BiOI was observed to be 10 %, 30 %, and 10 % respectively.

The concentration of generated ROSs should depend on the dosage of H_2O_2, and thus the effect of H_2O_2 concentration on the Fenton-like degradation of BPA was investigated. As shown in Fig. 3c, the Fenton-like degradation efficiency of BPA dramatically increased with the increase of H_2O_2 concentration from 1 to 40 mM. Nearly 90 % of BPA could be removed within 30 min by adding only 1 mM H_2O_2. With the dosage of H_2O_2 increased to 2 mM, BPA could be completely removed within 20 min. When 40 mM H_2O_2 was introduced, complete degradation of BPA occurred within a mere 2 min, highlighting the remarkable catalytic efficiency of the BiOI Fenton-like system. At high concentrations of H_2O_2, a substantial amount of ROS is generated to effectively target and oxidize BPA, thereby enhancing the speed and efficiency of the Fenton-like catalytic reaction. In this study, 2 mM H_2O_2 was employed to optimize the degradation conditions resembling Fenton reactions.

The effect of initial BPA concentration on Fenton-like degradation performance was further investigated, and the results are shown in Fig. 3d. When BPA concentration was below 20 $mg{\cdot}L^{-1}$, BPA could be completely removed within 30 min, indicating excellent Fenton-like catalytic performance for BiOI. With further increasing BPA concentration, the degradation efficiency of BiOI decreased significantly due to high concentrations of BPA would rapidly deplete the ROSs produced by BiOI Fenton-like system [22].

3.3. Activation mechanism of H_2O_2 to $\bullet O_2^-$ by BiOI

To clarify the role of ROSs for BPA removal, quenching experiments were performed by adding different scavengers to BiOI Fenton-like system. As shown in Fig. 4a, isopropanol (IPA), Tert-butanol (TBA), L-histidine, and p-benzoquinone (BQ) was used to quench $\bullet OH_{bulk}$ ($\bullet OH$ in solution), total $\bullet OH$ ($\bullet OH$ in solution and $\bullet OH$ adsorbed on the surface of BiOI), $^1O_2$, and $\bullet O_2^-$, respectively. Ar was aerated in solution to remove O_2 [5,23]. Without the addition of any scavengers, BPA can be completely degraded within only 20 min. With addition of TBA, IPA, and L-histidine, only a sight inhibitory effect for the degradation of BPA is

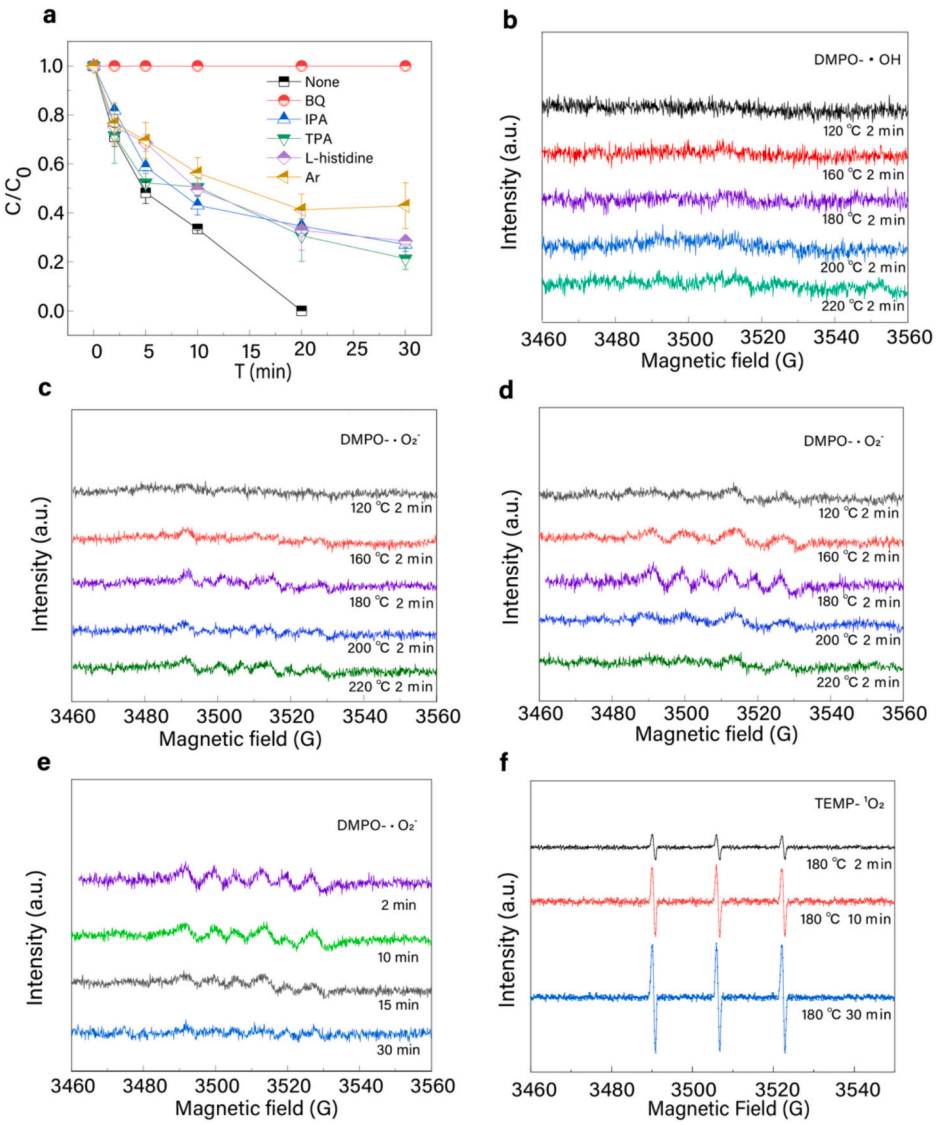

Fig. 4. (a) The Fenton-like catalytic degradation of BPA at initial pH = 5 by BiOI synthesized at 180 °C with different scavengers (10 mmol/L); (b) DMPO spin-trapping ESR spectra of •OH for the catalysts synthesized at different solvothermal temperatures with adding H_2O_2; (c) DMPO spin-trapping ESR spectra of $•O_2^-$ for the catalysts synthesized at different solvothermal temperatures without adding H_2O_2; (d) DMPO spin-trapping ESR spectra of $•O_2^-$ for the catalysts synthesized at different solvothermal temperatures with adding H_2O_2; (e) DMPO spin-trapping ESR spectra of $•O_2^-$ recording at different reaction time for the BiOI synthesized at 180 °C with adding H_2O_2; (f) TEMP spin-trapping ESR spectra of $^1O_2$ recording at different reaction time for the BiOI synthesized at 180 °C with adding H_2O_2.

observed, indicating that •OH and $^1O_2$ play minor role in degradation of BPA. Nevertheless, the degradation of BPA was completely inhibited with the addition of BQ, and no BPA could be degraded after 30 min. Meanwhile, the degradation efficiency of BPA was 50.1 % when Ar was introduced into the system, indicating O_2 was also an important contributor to the degradation of BPA. O_2 might promote the generation of $•O_2^-$ and thus involve the degradation process of BPA. The findings indicate that $•O_2^-$ was the primary ROS accountable for the Fenton-like catalytic disintegration of BPA.

To reveal the mechanism of H_2O_2 activation by BiOI, in situ ESR tests were used to detect the generated ROSs by using 5,5-dimethyl-L-pyrroline-N-oxide (DMPO) as a spin trapper to verify the existence of •OH and $•O_2^-$. 4-amino-2,2,6,6-tetramethylpiperidine (TEMP) was used as a spin-capture agent for $^1O_2$. As shown in Fig. 4b, after the addition of H_2O_2 for 2 min, the signal peaks related to DMPO-•OH in all samples synthesized at different temperatures were found to be negligible. This observation indicates that no •OH radicals were generated within the Fenton-like catalytic system of BiOI. As shown in Fig. 4c, no obvious ESR signal of DMPO-$•O_2^-$ adducts was observed when no H_2O_2 was added, which indicated that BiOI itself cannot produce $•O_2^-$ and the electron-poor reactive centers of Bi^{3+} on BiOI could adsorb and activate H_2O_2 and O_2 to generate $•O_2^-$. It is evident from Fig. 4d that the addition of H_2O_2 to samples synthesized at 160 and 180 °C results in the clear observation of six distinct ESR characteristic peaks corresponding to the DMPO-$•O_2^-$ radical, confirming the generation of $•O_2^-$ radicals. Notably, these radicals are only formed in the presence of both H_2O_2 and BiOI. The samples prepared at 180 °C exhibit the most pronounced ESR signal peaks for the DMPO-$•O_2^-$ radicals, indicating the highest productivity of $•O_2^-$ and strongest activation ability for H_2O_2. Furthermore, the evolution of the DMPO-$•O_2^-$ signal along with the reaction time in the BiOI/H_2O_2 system was also investigated (Fig. 4e). The intensities of the signal peak of DMPO-$•O_2^-$ increased firstly, and then decreased with the prolongation of the reaction time, implying the continuous production and consumption of $•O_2^-$ due to the activation and dissociation of H_2O_2 during the Fenton-like catalytic reactions. As shown in Fig. 4f, a triple-state signal with an intensity ratio of 1:1:1could be observed in the system containing both H_2O_2 and BiOI (T-180), confirming the presence of $^1O_2$. The intensities of the signal peak of TEMP-$^1O_2$ increased with the

prolongation of the reaction time, indicating the continuous production of $^1O_2$ during the Fenton-like catalytic reactions. These results demonstrate the generation of $\bullet O_2^-$ and $^1O_2$ in the Fenton-like process on BiOI. Combined with the results of quenching experiments, it can be concluded that although there is a significant amount of $^1O_2$ present in the Fenton-like system, the $^1O_2$ seemed to play a minor role in BPA removal. Thus, the highly efficient decomposition of BPA is likely attributed to the continuous generation of $\bullet O_2^-$ from H_2O_2. It can be inferred that $^1O_2$ does not play a major role in this process, and the $^1O_2$ is formed through the conversion of $\bullet O_2^-$ in the absence of BPA. To the best of our knowledge, it is the first time to report that the selective activation of H_2O_2 to $\bullet O_2^-$ by BiOI in dark for pollutant degradation. As shown in Fig. 3b, solution initial pH played a crucial role in the Fenton-like degradation of BPA. At low pH, a strong acidic condition could markedly inhibit the generation of $\bullet O_2^-$ radical and decreases the Fenton-like catalytic activity BiOI, which might be ascribed to the excessive H^+ hindering the effective contact between the BiOI surface and H_2O_2. At high pH, H_2O_2 could be preferently decomposed into H_2O and O_2 without producing $\bullet O_2^-$, which would decrease the amount of H_2O_2 in the solution and significantly inhibit the removal efficiency of BPA.

To better understand the overall Fenton-like process, XPS spectra and XRD spectra of fresh and used BiOI were used to explore the changes in the crystal phase composition and chemical valence states during the Fenton-like reaction. As shown in Fig. 5a, the diffraction peaks of metallic Bi disappeared after activation of H_2O_2, indicating that the presence of small amounts of metallic Bi in the BiOI structure could promote the activation of H_2O_2 to $\bullet O_2^-$. Furthermore, XRD patterns of BiOI showed no significant change compared with the original BiOI. In Fig. 5b, two peaks were located at 159.5 and 164.9 eV from the Bi $4f_{7/2}$ and Bi $4f_{5/2}$ of fresh BiOI, corresponding to Bi^{3+}. After adding H_2O_2, the peaks of Bi $4f_{7/2}$ and Bi $4f_{5/2}$ shifted to a low binding energy of 159.3 and 164.6 eV, respectively, indicating an increase in electron density, corresponding to lower oxidation states of Bi ($Bi^{(3-x)+}$). The shift of the XPS peaks implied that electron transfer occurred between H_2O_2 and the active sites on the surface of BiOI, in which Bi^{3+} may gain the electrons from H_2O_2, leading to an increase of generate $Bi^{(3-x)+}$. After being used, the peak intensities and positions of I $3d_{5/2}$ and I $3d_{3/2}$ in BiOI (Fig. 5c) had no significant change. At the same time, compared to pristine BiOI, the O 1s spectra showed that the peak area of the chemisorbed oxygen at 533.2 eV (Fig. 5d) for the BiOI increased prominently after the addition of H_2O_2, and the peak of O—H bond shifted from 531.7 to 531.5 eV, corroborating that oxygen vacancies (O_V) might be formed after the addition of H_2O_2, which could also lead to the negative shift of peaks of Bi and I due to the loss of an oxygen atom from the surface of BiOI can increase the electron cloud density around Bi and I.

Based on the above results of quenching experiments, ESR and XPS, a scientifically plausible activation mechanism of H_2O_2 and a feasible pathway for the generation of $\bullet O_2^-$ by the BiOI Fenton-like catalytic system are reasonably proposed as depicted in Scheme 1. Firstly, H_2O_2 can provide electrons to react with electron-poor reactive center of Bi^{3+} sites on the surface of BiOI to generate a large number of $\bullet O_2^-$ [21,24] similar to homogeneous Fenton reaction, simultaneously leading to the generation of electron-rich reactive centers ($Bi^{(3-x)+}$). Then, the presence of a large number of localized electrons on the electron-rich reactive centers could effectively reduce dissolved O_2 to synergistically produce $\bullet O_2^-$ [21,24], and thus play an important role in Fenton-like catalytic reactions [25]. $\bullet O_2^-$ might be weakly adsorbed on the BiOI surface and released from the surface of BiOI to further react with BPA. It should be noted that the generation of $\bullet O_2^-$ [21,24] through the activation of H_2O_2 or O_2 can also lead to the inactivation of active sites on the surface of BiOI, resulting in a reduction in the number of active sites during the progression of the reaction. The findings demonstrated that BiOI effectively functions as an electron-poor reactive center of Bi^{3+} to activate H_2O_2 to $\bullet O_2^-$, while simultaneously generating an electron-rich reactive center ($Bi^{(3-x)+}$) for the reduction of dissolved O_2 to $\bullet O_2^-$. Therefore, the synergistic effect of electron-rich and electron-poor dual reactive centers on the surface of BiOI effectively promotes the chemical reactivity of BiOI and the decomposition of H_2O_2, and thus greatly improving the generation of $\bullet O_2^-$ for highly effective Fenton-like catalytic degradation of BPA [11]. In addition, $\bullet O_2^-$ could be further converted to $^1O_2$ in the

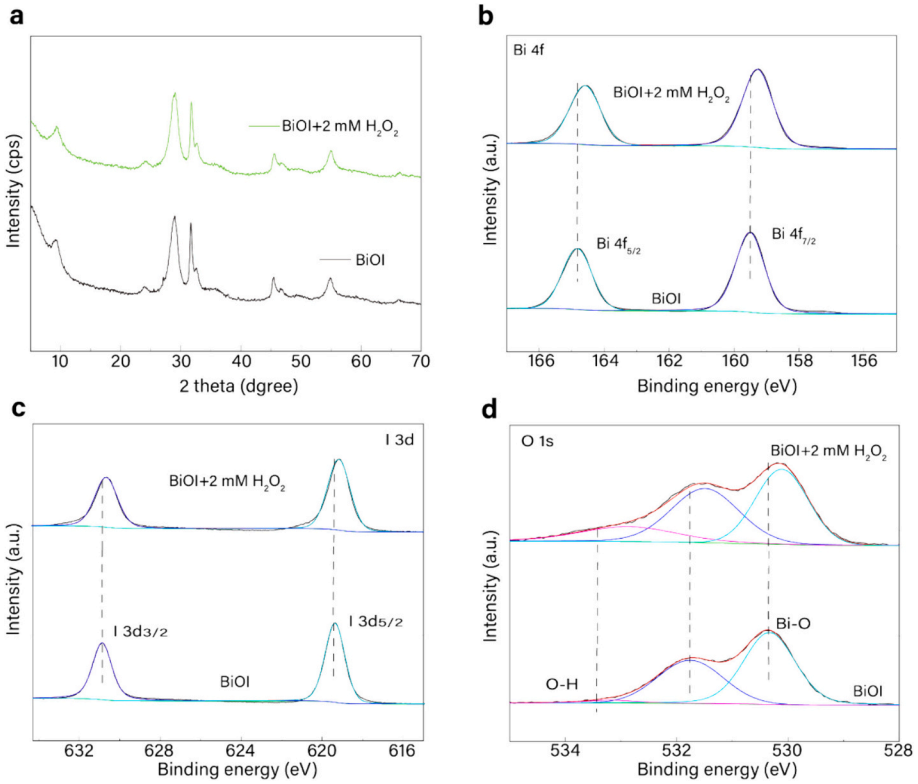

Fig. 5. XRD spectra (a), XPS spectra of Bi 4f (b), I 3d (c), and O 1s (d) for the optimized BiOI before and after reaction with H_2O_2.

absence of BPA. The activation process of H_2O_2 or O_2 and relative mechanism can be described as below:

$$Bi^{3+} + H_2O_2 \rightarrow Bi^{(3-x)+} + \bullet HO_2 + H^+ \quad (1)$$

$$\bullet HO_2 \rightarrow H^+ + \bullet O_2^- \quad (2)$$

$$Bi^{(3-x)+} + O_2 \rightarrow Bi^{3+} + \bullet O_2^- \quad (3)$$

$$2 \bullet O_2^- + 2\,H_2O \rightarrow {}^1O_2 + H_2O_2 + 2 \bullet OH \quad (4)$$

Besides, the reusability and stability of the BiOI was evaluated (Fig. S2). The removal efficiency of BPA within 30 min slightly decreased with increasing number of cycles (5), and the removal efficiencies for BPA were 100 %, 44 %, 12 %, 9 % and 0 % at the end of each cycle. After the Fenton-like catalytic reaction, about 4.68 and 0.02 ppm of I^- and Bi^{3+} in the solution could be detected (Fig. S3), respectively. This implies that the leaching of I^- from the surface of BiOI leads to the decreased Fenton-like catalytic activity of the BiOI.

3.4. Effect of coexisting halide ions and natural organic matter on the degradation process of BPA

Halide ions are ubiquitous in estuarine and coastal waters, and thus may affect the transport, transformation, and fate of pollutants [5]. In order to better understand the effect of adding halide ions on the Fenton-like degradation process of BPA by BiOI, various commonly used halides (NaF, NaCl and NaBr) with a series of concentrations (0 to 100 mM) were added to the solution. The addition of NaF had no significant effect on the removal of BPA (Fig. 6a). As the NaF concentration increased, there was a slight decrease in degradation rate. However, even with the addition of 100 mM NaF, the degradation efficiency of BPA could still reach approximately 70 % within just 30 min. As depicted in Fig. 6b and c, the addition of low concentrations (0–10 mM) of NaCl and NaBr did not have a significant impact on the removal efficiency of BPA. However, higher concentrations of NaCl or NaBr exhibited notable inhibitory effects on BPA degradation, leading to a significant decrease in the efficiency of BPA degradation as the concentration of NaCl or NaBr increased. For instance, the degradation efficiency of BPA reached approximately 60 % within 30 min upon addition of 100 mM NaCl. And when the concentration of NaBr was increased to 10 mM and 100 mM,

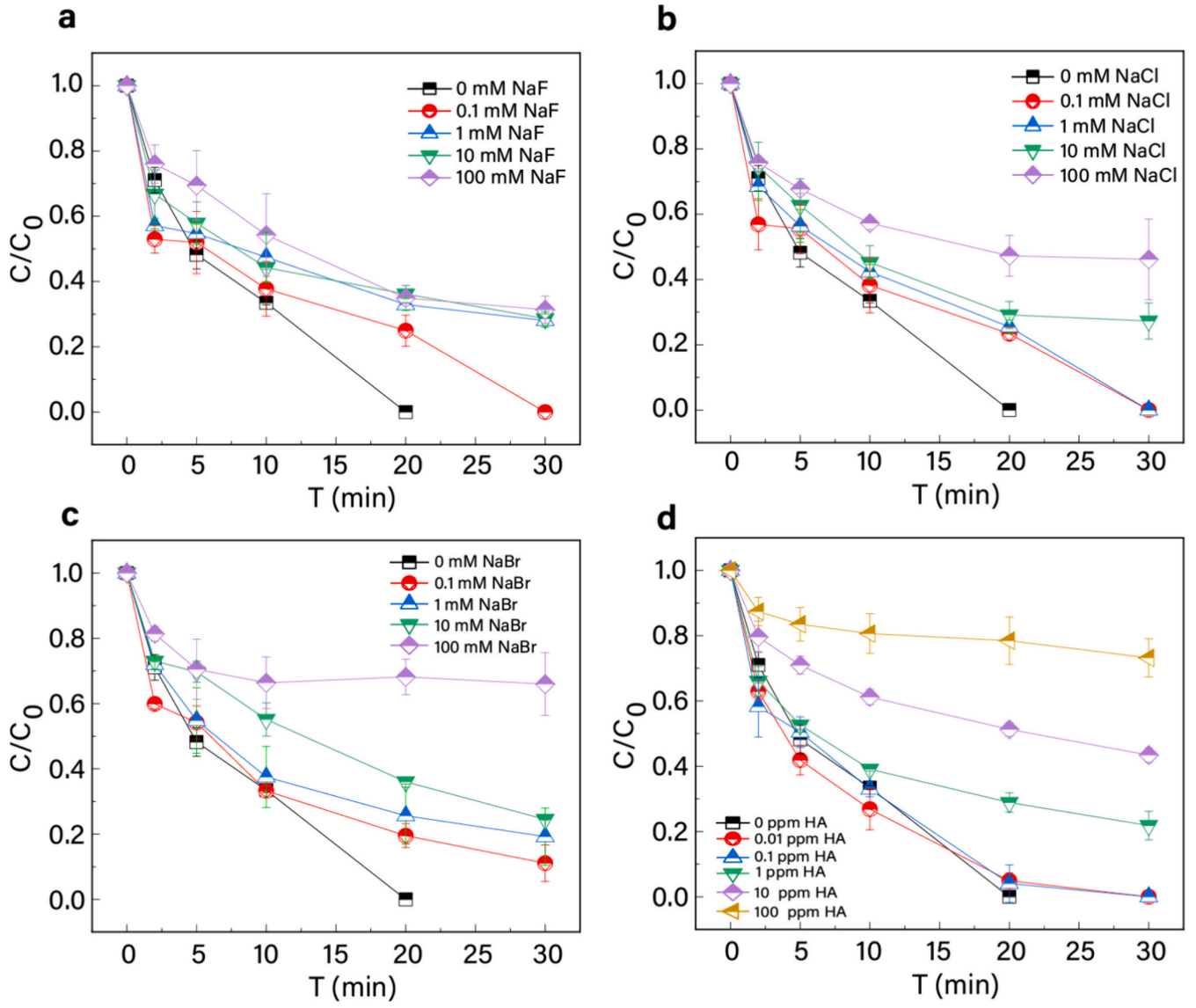

Fig. 6. The Fenton-like catalytic degradation of BPA by BiOI synthesized at 180 °C at initial pH = 5 with different concentrations of NaF (a), NaCl (b), NaBr (c), and HA (d).

only around 70 % and 30 % of BPA were respectively eliminated after the same time period. This suggests that NaCl and NaBr could inhibit the Fenton-like catalytic activity of BiOI when the concentration of NaCl and NaBr is greater than 100 and 10 mM, respectively. NaBr suppressed the degradation efficiency of BPA more efficiently than NaCl. The decreased degradation efficiencies of BPA in the presence of halide ions imply that the concentration of the main ROSs for BPA degradation might be reduced. This phenomenon can be attributed to the fact that excessive Br^- could react with H_2O_2 to form Br_2. However, Br_2 is unable to react with BPA, leading to a significant decrease in H_2O_2 concentration and inhibition of BPA degradation. Furthermore, the reduced efficiency of Fenton-like degradation for BPA in the presence of halide ions might be caused by competition between these ions and BPA for active sites on the surface of BiOI. Moreover, Natural organic matter (NOM), as an essential

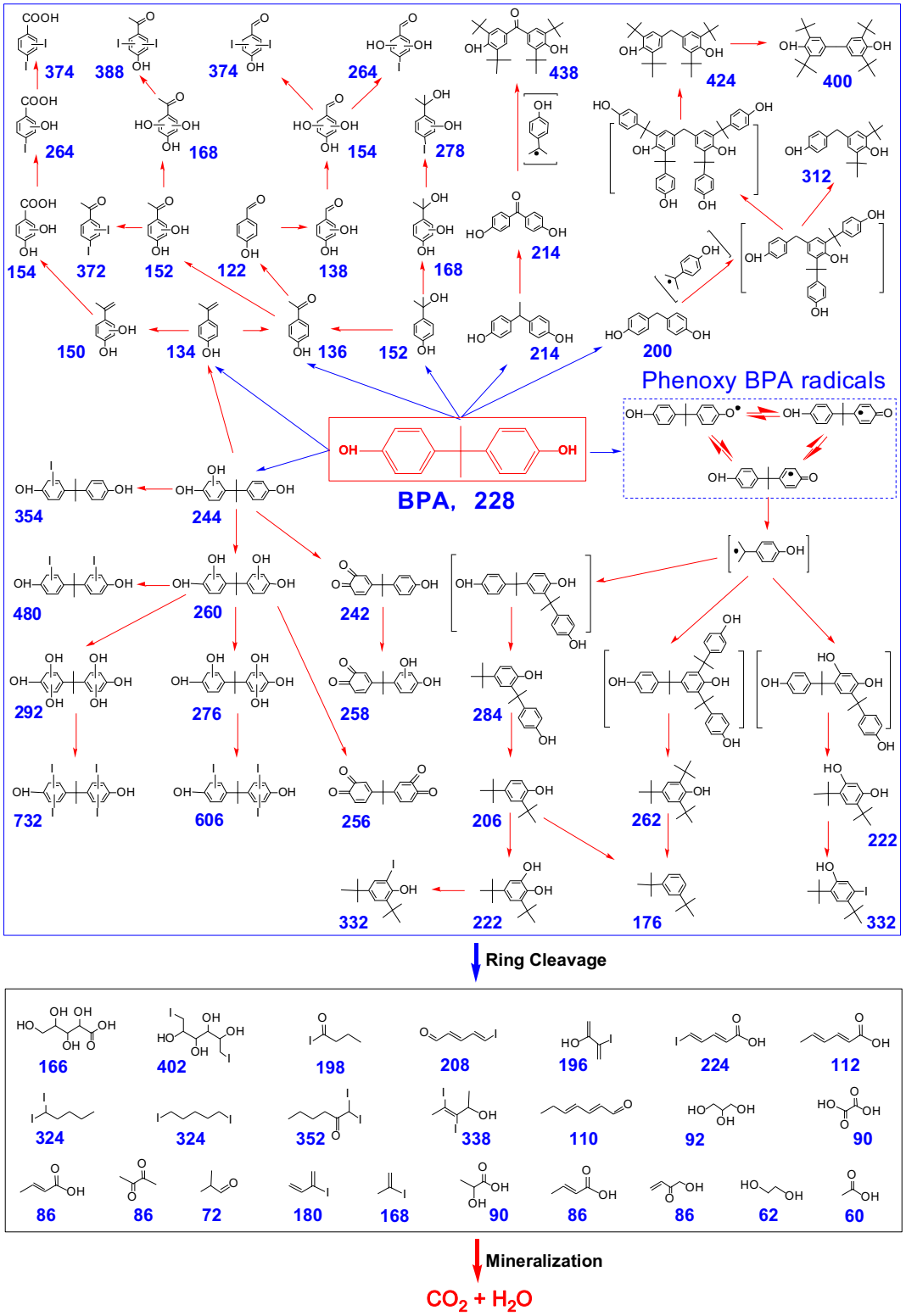

Fig. 7. Possible catalytic degradation pathways of BPA in BiOI Fenton-like catalytic system.

component in water, universally exists in various natural water and wastewaters, and consequently might affect the removal of organic pollutants in real aquatic environments [11]. Herein, humic acid (HA) was selected as a surrogate to NOM to evaluate the influence of NOM. As shown in Fig. 6d, the presence of HA exhibited minimal inhibitory effects on the removal efficiency of BPA, even when the HA concentration reached 10 ppm. The aqueous concentrations of I^- and Bi^{3+} as a function of stirring time for suspensions containing BiOI synthesized at 180 °C during the reaction process were measured in the presence and absence of humic acids at initial pH = 5 (Fig. S3). The aqueous concentration of I^- in the solution increased with stirring time, suggesting the leaching and dissolution of BiOI surface. Furthermore, the concentrations of dissolved I^- decreased with increasing humic acids concentrations from 0 to 100 ppm. The concentration of dissolved I^- in the absence of humic acids (pure water) was remarkable higher than the system in the presence of humic acids. Regardless of the presence or absence of humic acids, the aqueous concentrations of Bi^{3+} were significantly lower than those of dissolved I^-, indicating that humic acids could act as metal chelating agents with BiOI surface and hinder the leaching and dissolution of BiOI surface. Furthermore, high concentration of humic acids (100 ppm) may also hinder the reaction between BiOI surface and H_2O_2, resulting in the decreased Fenton-like catalytic degradation of BPA. Based on the above findings, it can be concluded that the BiOI Fenton-like catalytic system holds great promise for the treatment of natural water and wastewater. Moreover, it represents a viable and sustainable alternative for effectively degrading organic pollutants.

3.5. Intermediate identification and catalytic degradation mechanism of BPA

To elucidate the degradation pathway of BPA, identification of intermediate products formed during Fenton-like degradation process of BPA by BiOI was determined by HPLC-MS. Fig. S4 shows the HPLC chromatograms of BPA degradation at different times. For untreated samples, an absorption peak of original BPA molecule with a retention time (t_R) of 8.66 min could be observed. After 2 min of reaction, the BPA concentration significantly decreased. Simultaneously, five degradation intermediates (P1 with t_R 4.4 min, P2 with t_R 5.82 min, P3 with t_R 5.97 min, P4 with t_R 8.87 min, and P5 with t_R 9.30 min) were detected. As the reaction time continued, all of the peaks of BPA and five intermediates decreased gradually. After 20 min of treatment, the BPA peak decreased to below the detection limit. The main intermediates, P1, P2, P3, P4 and P5 with molecular weight of 732, 480, 606, 354 and 480, were identified from MS data, and all of the five intermediates were iodine substitution products of BPA. Furthermore, several intermediates were also detected using HPLC-MS in negative and positive ion modes, respectively. It is worth mentioning that novel intermediates with iodine substitution were identified for the first time. According to the identified intermediate products and the previous reports in literature [21,26,27], the possible degradation pathways of BPA were proposed and displayed in Fig. 7. It should be noted that the products marked by a square bracket were not detected in this study but probably existed during Fenton-like degradation process. The C−C single bond between the phenyl group and isopropyl carbon would be susceptibly attacked by $\bullet O_2^-$ because its higher frontier electron density, resulting in its β-scission. $\bullet O_2^-$ could abstract •H species from BPA to form three resonance stabilized phenoxy BPA radicals, which will be involved in a series of reactions including successive hydroxylation, dehydrogenation, alkylic-oxidation, radical coupling, and bond cleavage to form various products. Furthermore, β-scission of BPA or phenoxy BPA radical could produce isopropylphenol radical, isopropylphenol cation, and phenol radical [28]. These radicals can also react with various intermediates to form various molecules with small relative molecular masses and even BPA oligomers with large relative molecular masses. Further degradation results in the formation of aromatic ring opening products and smaller molecules. Of note, the hydroxyl groups of various hydroxylation intermediates could also be substituted by iodine originated from the leakage of iodine from BiOI.

4. Conclusions

In the present work, a light-free Fenton-like catalyst consisting of the flower-like BiOI micro-spherulites was successfully prepared using a solvothermal method. BiOI could synchronously act as electron-poor reactive center of Bi^{3+} to activate H_2O_2 to $\bullet O_2^-$ and in situ generate electron-rich reactive center ($Bi^{(3-x)+}$) to reduce dissolved O_2 to $\bullet O_2^-$. The synergistic effect of electron-rich and electron-poor dual reactive centers on the surface of BiOI effectively promoted the chemical reactivity of BiOI and the decomposition of H_2O_2, and thus greatly improving the generation of $\bullet O_2^-$ for highly effective Fenton-like catalytic degradation of BPA. $\bullet O_2^-$ was the only ROS responsible for highly effective Fenton-like catalytic degradation of BPA. The removal efficiency of BPA exhibited significant pH dependence. Moreover, the presence of low concentration of halide ions or HA only exerted minimal inhibitory effects on the removal efficiency of BPA. Additionally, several intermediates were identified and the possible degradation pathways of BPA were proposed during the catalytic degradation of BPA. This study indicated that the BiOI Fenton-like catalytic system holds great promise as highly promising materials for natural water and wastewater treatment, and it presents an efficient and sustainable alternative for degrading organic pollutants.

CRediT authorship contribution statement

Jinghao Huo: Writing – original draft, Methodology, Investigation, Formal analysis. **Xin Nie:** Writing – review & editing, Validation, Data curation, Conceptualization. **Yanfei Yin:** Data curation. **Quan Wan:** Supervision, Conceptualization. **Jukun Xiong:** Data curation. **Huixian Shi:** Writing – review & editing, Supervision, Conceptualization.

Declaration of competing interest

The authors declare that they have no known competing financial interests or personal relationships that could have appeared to influence the work reported in this paper.

Data availability

Data will be made available on request.

Acknowledgements

This work was financially supported by Guizhou Provincial Science and Technology projects ([2020]1Z039), National Natural Science Foundation of China (41902041), the Open Research Fund Program of Collaborative Innovation Center for Molecular Imaging of Precision Medicine (2020-ZD01, 2023-ZD01), National Natural Science Foundation of China (41991312).

Appendix A. Supplementary data

Supplementary data to this article can be found online at https://doi.org/10.1016/j.jwpe.2024.105744.

References

[1] C. Chang, L. Zhu, Y. Fu, X. Chu, Highly active Bi/BiOI composite synthesized by one-step reaction and its capacity to degrade bisphenol a under simulated solar light irradiation, Chem. Eng. J. 233 (2013) 305–314, https://doi.org/10.1016/j.cej.2013.08.048.

[2] R. Ma, S. Zhang, X. Liu, M. Sun, J. Cao, J. Wang, S. Wang, T. Wen, X. Wang, Oxygen defects-induced charge transfer in $Bi_7O_9I_3$ for enhancing oxygen activation and

visible-light degradation of BPA, Chemosphere 286 (2022) 131783, https://doi.org/10.1016/j.chemosphere.2021.131783.
[3] L. Wang, D. Yan, L. yu, C. Hu, N. Jiang, L. Zhang, Notable light-free catalytic activity for pollutant destruction over flower-like BiOI microspheres by a dual-reaction-center Fenton-like process, J. Colloid Interface Sci. 527 (2018) 251–259, https://doi.org/10.1016/j.jcis.2018.05.055.
[4] C. Zhang, W. Fei, H. Wang, N. Li, D. Chen, Q. Xu, H. Li, J. He, J. Lu, P-n heterojunction of BiOI/ZnO nanorod arrays for piezo-photocatalytic degradation of bisphenol an in water, J. Hazard. Mater. 399 (2020) 123109, https://doi.org/10.1016/j.jhazmat.2020.123109.
[5] X. Nie, G. Li, S. Li, Y. Luo, W. Luo, Q. Wan, T. An, Highly efficient adsorption and catalytic degradation of ciprofloxacin by a novel heterogeneous Fenton catalyst of hexapod-like pyrite nanosheets mineral clusters, Appl. Catal. B Environ. 300 (2022) 120734, https://doi.org/10.1016/j.apcatb.2021.120734.
[6] B. Jain, A. Sing, H. Kim, E. Lichtfouse, V.K. Sharma, Treatment of organic pollutants by homogeneous and heterogeneous Fenton reaction processes, Environ. Chem. Lett. 16 (2018) 947–967, https://doi.org/10.1007/s10311-018-0738-3.
[7] L. yu, L. Zhang, C. Hu, Enhanced Fenton-like degradation of pharmaceuticals over framework copper species in copper-doped mesoporous silica microspheres, Chem. Eng. J. 274 (2015) 298–306, https://doi.org/10.1016/j.cej.2015.03.137.
[8] A. Karci, I. Arslan-Alaton, T. Olmez-Hanci, M. Bekbölet, Transformation of 2,4-dichlorophenol by H_2O_2/UV-C, Fenton and photo-Fenton processes: oxidation products and toxicity evolution, J. Photochem. Photobiol. A. 230 (2012) 65–73, https://doi.org/10.1016/j.jphotochem.2012.01.003.
[9] Q. Li, J. Ren, Y. Hao, Y. Li, X. Wang, Y. Liu, R. Su, F. Li, Insight into reactive species-dependent photocatalytic toluene mineralization and deactivation pathways via modifying hydroxyl groups and oxygen vacancies on BiOCl, Appl. Catal. B Environ. 317 (2022) 121761, https://doi.org/10.1016/j.apcatb.2022.121761.
[10] H. Li, J. Shang, Z. Yang, W. Shen, Z. Ai, L. Zhang, Oxygen vacancy associated surface Fenton chemistry: surface structure dependent hydroxyl radicals generation and substrate dependent reactivity, Environ. Sci. Technol. 51 (2017) 5685–5694, https://doi.org/10.1021/acs.est.7b00040.
[11] W. Qu, C. Chen, Z. Tang, D. Xia, D. Ma, Y. Huang, Q. Lian, C. He, D. Shu, B. Han, Electron-rich/poor reaction sites enable ultrafast confining Fenton-like processes in facet-engineered BiOI membranes for water purification, Appl. Catal. B Environ. 304 (2022) 120970, https://doi.org/10.1016/j.apcatb.2021.120970.
[12] K. Wang, S. Zeng, G. Li, Y. Dong, Q. Wang, L. Zhang, Z. Ren, P. Wang, Superoxide radical induced redox processes for simultaneous reduction of Cr(VI) and oxidation of ciprofloxacin in wastewater, Appl. Catal. B Environ. 343 (2024) 123565, https://doi.org/10.1016/j.apcatb.2023.123565.
[13] Y. Qi, J. Zhao, H. Wang, A. Zhang, J. Li, M. Yan, T. Guo, Shaddock peel-derived n-doped carbon quantum dots coupled with ultrathin BiOBr square nanosheets with boosted visible light response for high-efficiency photodegradation of RhB, Environ. Pollut. 325 (2023) 121424, https://doi.org/10.1016/j.envpol.2023.121424.
[14] S. Wang, D. Song, L. Liao, M. Li, Z. Li, W. Zhou, Surface and interface engineering of BiOCl nanomaterials and their photocatalytic applications, Adv. Colloid Interf. Sci. 324 (2024) 103088, https://doi.org/10.1016/j.cis.2024.103088.
[15] Y. Sun, C. Zeng, X. Zhang, Z. Zhang, B. Yang, S. Guo, Tendencies of alloyed engineering in BiOX-based photocatalysts: a state-of-the-art review, Rare Metals (2024) 1–25, https://doi.org/10.1007/s12598-023-02569-6.
[16] Z. Saddique, M. Imran, A. Javaid, S. Latif, N. Hussain, P. Kowal, G. Boczkaj, Band engineering of BiOBr based materials for photocatalytic wastewater treatment via advanced oxidation processes (AOPs) – A review, Water Resour. Ind. 29 (2023), https://doi.org/10.1016/j.wri.2023.100211.
[17] N. Talreja, S. Afreen, M. Ashfaq, D. Chauhan, A.C. Mera, C.A. Rodríguez, R. V. Mangalaraja, Bimetal (Fe/Zn) doped BiOI photocatalyst: an effective photodegradation of tetracycline and bacteria, Chemosphere 280 (2021) 130803, https://doi.org/10.1016/j.chemosphere.2021.130803.
[18] L. Chen, C. Li, Y. Zhao, J. Wu, X. Li, Z. Qiao, P. He, X. Qi, Z. Liu, G. Wei, Constructing 3D Bi/$Bi_4O_5I_2$ microspheres with rich oxygen vacancies by one-pot solvothermal method for enhancing photocatalytic activity on mercury removal, Chem. Eng. J. 425 (2021) 131599, https://doi.org/10.1016/j.cej.2021.131599.
[19] J. Wang, Y. Wang, C. Cao, Y. Zhang, Y. Zhang, L. Zhu, Decomposition of highly persistent perfluorooctanoic acid by hollow Bi/$BiOI_{1-x}F_x$: synergistic effects of surface plasmon resonance and modified band structures, J. Hazard. Mater. 402 (2021) 123459, https://doi.org/10.1016/j.jhazmat.2020.123459.
[20] Q. Li, S. Gao, J. Hu, H. Wang, Z. Wu, Superior NOx photocatalytic removal over hybrid hierarchical Bi/BiOI with high non-NO_2 selectivity: synergistic effect of oxygen vacancies and bismuth nanoparticles, Catal, Sci. Technol. 8 (2018) 5270–5279, https://doi.org/10.1039/c8cy01466c.
[21] W. Qu, H. Wen, X. Qu, Y. Guo, L. Hu, W. Liu, S. Tian, C. He, D. Shu, Enhanced Fenton-like catalysis for pollutants removal via MOF-derived $Co_xFe_{3-x}O_4$ membrane: oxygen vacancy-mediated mechanism, Chemosphere 303 (2022) 135301, https://doi.org/10.1016/j.chemosphere.2022.135301.
[22] J. Wang, C. Cao, Y. Wang, Y. Wang, B. Sun, L. Zhu, In situ preparation of p-n BiOI@Bi_5O_7I heterojunction for enhanced pfoa photocatalytic degradation under simulated solar light irradiation, Chem. Eng. J. 391 (2020) 123530, https://doi.org/10.1016/j.cej.2019.123530.
[23] W. An, H. Wang, T. Yang, J. Xu, Y. Wang, D. Liu, J. Hu, W. Cui, Y. Liang, Enriched photocatalysis-Fenton synergistic degradation of organic pollutants and coking wastewater via surface oxygen vacancies over Fe-BiOBr composites, Chem. Eng. J. 451 (2023) 138653, https://doi.org/10.1016/j.cej.2022.138653.
[24] C. Zhang, Y. Deng, Q. Wan, H. Zeng, H. Wang, H. Yu, H. Pang, W. Zhang, X. Yuan, J. Huang, Built-in electric field boosted exciton dissociation in sulfur doped BiOCl with abundant oxygen vacancies for transforming the pathway of molecular oxygen activation, Appl. Catal. B Environ. 343 (2024) 123557, https://doi.org/10.1016/j.apcatb.2023.123557.
[25] J. Zheng, L. Li, Z. Dai, Y. Tian, T. Fang, S. Xin, B. Zhu, Z. Liu, L. Nie, A novel Fenton-like catalyst of Ag_3PO_4/G-C_3N_4: its performance and mechanism for tetracycline hydrochloride degradation in dark, Appl. Surf. Sci. 571 (2022) 151305, https://doi.org/10.1016/j.apsusc.2021.151305.
[26] X. Lin, K. Shih, J. Chen, X. Xie, Y. Zhang, Y. Chen, Z. Chen, Y. Li, Insight into flower-like greigite-based peroxydisulfate activation for effective bisphenol an abatement: performance and electron transfer mechanism, Chem. Eng. J. 391 (2020) 123558, https://doi.org/10.1016/j.cej.2019.123558.
[27] Y. Guo, W. Shi, Y. Zhu, Y. Xu, F. Cui, Enhanced photoactivity and oxidizing ability simultaneously via internal electric field and valence band position by crystal structure of bismuth oxyiodide, Appl. Catal. B Environ. 262 (2020) 118262, https://doi.org/10.1016/j.apcatb.2019.118262.
[28] D. Roy, S. Neogi, S. De, Mechanistic investigation of photocatalytic degradation of bisphenol-a using mil-88a (Fe)/MoS_2 z-scheme heterojunction composite assisted peroxymonosulfate activation, Chem. Eng. J. 428 (2022) 131028, https://doi.org/10.1016/j.cej.2021.131028.